Photoproduction of the B_c meson at future e^+e^- colliders

Xi-Jie Zhan[*], Xing-Gang Wu,[†] and Xu-Chang Zheng[‡]

Department of Physics, Chongqing Key Laboratory for Strongly Coupled Physics, Chongqing University, Chongqing 401331, People's Republic China

In the present paper we study the photoproduction of various S-wave B_c states, i.e., $B_c(1^1S_0)$, $B_c^*(1^1S_0)$, $B_c(2^1S_0)$, and $B_c^*(2^3S_1)$, at future e^+e^- colliders within the framework of nonrelativistic QCD. Two sources of the initial photons can be realized in the production, i.e., the laser backscattering photon and the Weizäcker-Williams approximation photon. In addition to the direct photoproduction via the subprocess, $\gamma + \gamma \to B_c + b + \bar{c}$, we also calculate the resolved photoproduction via the subprocesses, $\gamma + g \to B_c + b + \bar{c}$ and $q + \bar{q} \to B_c + b + \bar{c}$ with $q = u, d, s, g$, respectively. Numerical results indicate that the contributions from the single resolved photoproduction are significant and even dominant at certain collision configuration. At the future high-energy and high-luminosity e^+e^- colliders, the B_c meson generated via the photoproduction mechanism is promisingly observable and can be well studied.

I. INTRODUCTION

The $B_c(1^1S_0)$ meson, including its excited states, are strong interaction systems composed of two heavy quarks with different flavors. This unique flavored bound-state system could be a good probe for studying the strong interaction among quarks and gluons, and the QCD. So far the B_c mesons have been only observed at the hadronic colliders. Its ground state was discovered in 1998 by the CDF Collaboration [1,2], and its excited $2S$ states were observed by ATLAS Collaboration [3] in 2014 and by the CMS and LHCb Collaborations [4,5] in 2019. Many theoretical studies have been done for B_c production at hadron colliders [6–25]. A computer program, BCVEGPY, for the direct hadronic production of B_c meson was given in Refs. [19–21]. The next generation e^+e^- colliders were proposed by some groups, such as the FCC-ee [26], the CEPC [27,28], the ILC [29,30] and so on. These future e^+e^- colliders are planed to have the ability to run at several high collision energies with unprecedented luminosities. They are expected to be great platforms for many subjects including heavy quarkonium physics [31–41].

As for the B_c meson, there are two production modes at the e^+e^- collider, i.e., the production via the e^+e^-

annihilation [31,42–48] and the photoproduction mechanism [35,49,50]. A computer program, BEEC, for the first production mode has been presented in Refs. [42,48]. As for the photoproduction mechanism, the B_c meson can be produced via the photon-photon fusion such as $\gamma + \gamma \to B_c + b + \bar{c}$. Here the initial photons can come from the bremsstrahlung effect, whose energy spectrum are well described in the Weizäcker-Williams approximation (WWA) [51]; moreover, the laser backscattering (LBS) can also provide high-energy photon. In addition to the above direct photoproduction, there are also channels of resolved photoproduction, where the photons participate in the hard process via their quark and gluon content [52]. As a result, the process $e^+e^- \to e^+e^-B_c + X$ receives contributions from three channels, i.e., the direct, single-resolved and double-resolved photoproduction. All three channels should be considered in the calculation because they are of the same order in the perturbative expansion. The resolved photoproduction of heavy quarkonium have been investigated in some literature [39–41,52,53] and it is indicated that the single-resolved photoproduction can give significant or dominant contributions both in the color-singlet and color-octet channels. While for the B_c meson, only the direct photoproduction channel has been studied [35,49,50] and it is worthy and reasonable to investigate the effects of the resolved channels according to the previous studies.

In this work, based on the framework of nonrelativistic QCD (NRQCD) [54], we study the photoproduction of $B_c, B_c^*(1^3S_1)$, $B_c(2^1S_0)$ and $B_c^*(2^3S_1)$ at future e^+e^- colliders, considering two sources of the initial photons, i.e., the LBS photon and the WWA photon. In addition to the direct photoproduction $\gamma + \gamma \to B_c + b + \bar{c}$, we especially

[*]zhanxj@cqu.edu.cn
[†]wuxg@cqu.edu.cn
[‡]zhengxc@cqu.edu.cn

calculate the subprocesses of the resolved photoproduction, $\gamma + g \to B_c + b + \bar{c}$ and $q + \bar{q} \to B_c + b + \bar{c}$ with $q = u$, d, s, g, respectively. In Sec. II we present the formulation of our calculation. Numerical results and discussions are given in Sec. III and a brief summary is in Sec. IV.

II. FORMULATION

The energy spectrum of the photon from the bremsstrahlung effect can be described in WWA, which takes the form [51],

$$f_{\gamma/e}(x) = \frac{\alpha}{2\pi} \left[\frac{1 + (1-x)^2}{x} \log \frac{Q_{\max}^2}{Q_{\min}^2} \right.$$
$$\left. + 2m_e^2 x \left(\frac{1}{Q_{\max}^2} - \frac{1}{Q_{\min}^2} \right) \right], \tag{1}$$

where $x = E_\gamma/E_e$ is the fraction of the longitudinal momentum carried by the photon, α is the electromagnetic fine structure constant, $Q_{\min}^2 = m_e^2 x^2/(1-x)$ and $Q_{\max}^2 = (E\theta_c)^2(1-x) + Q_{\min}^2$. $\theta_c = 32$ mrad is the maximum scattered angular cut in order to ensure the photon to be real. $E = E_e = \sqrt{s}/2$ with the collision energy $\sqrt{s}$.

And for the case of LBS photon, its spectrum function is [55]

$$f_{\gamma/e}(x) = \frac{1}{N} \left[1 - x + \frac{1}{1-x} - 4r(1-r) \right], \tag{2}$$

where $r = x/[x_m(1-x)]$, and the normalization factor,

$$N = \left(1 - \frac{4}{x_m} - \frac{8}{x_m^2} \right) \log(1 + x_m) + \frac{1}{2} + \frac{8}{x_m} - \frac{1}{2(1+x_m)^2}. \tag{3}$$

Here $x_m = 4E_e E_l \cos^2 \frac{\theta}{2}$, E_e, and E_l are the energies of incident electron and laser beams, respectively. θ is the angle between them. The energy of the LBS photon is restricted by

$$0 \le x \le \frac{x_m}{1+x_m}, \tag{4}$$

with optimal value of x_m being 4.83 [56]. These two spectra have quite different behaviors as shown in Fig. 1.

Within the framework of NRQCD factorization, the cross section of B_c photoproduction at the e^+e^- collider can be factorized as [57]

$$d\sigma(e^+e^- \to e^+e^- B_c + b + \bar{c})$$
$$= \int dx_1 f_{\gamma/e}(x_1) \int dx_2 f_{\gamma/e}(x_2)$$
$$\times \sum_{i,j,k} \int dx_i f_{i/\gamma}(x_i) \int dx_j f_{j/\gamma}(x_j)$$
$$\times \sum_n d\hat{\sigma}(ij \to c\bar{b}[n] + b + \bar{c})\langle \mathcal{O}^{B_c}[n]\rangle. \tag{5}$$
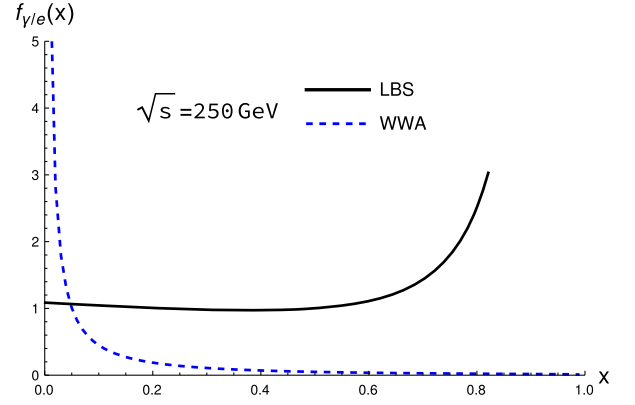

FIG. 1. The energy spectra of the LBS photon and the WWA photon.

Here $f_{i/\gamma}$ ($i = \gamma$, g, u, d, s) represents the Glück-Reya-Schienbein distribution function of parton i in photon [58]. $f_{\gamma/\gamma}(x) = \delta(1-x)$ is for the direct photoproduction process. $d\hat{\sigma}(ij \to c\bar{b}[n] + b + \bar{c})$ is the differential partonic cross section, which can be calculated perturbatively. $c\bar{b}[n]$ is the intermediate state with quantum number n. $\langle \mathcal{O}^{B_c}[n]\rangle$ is the long distance matrix element(LDME) representing the probability for a $c\bar{b}[n]$ pair hadronizing into B_c meson. In the lowest order approximation, only the color-singlet intermediate state $c\bar{b}[^1S_0^{[1]}]$ is considered and the corresponding LDME can be calculated by potential models. For definiteness, we consider the following subprocesses for three production channels,

$$\gamma + \gamma \to B_c(B_c^*, B_c(2^1S_0), B_c^*(2^3S_1)) + b + \bar{c}, \tag{6}$$

$$\gamma + g \to B_c(B_c^*, B_c(2^1S_0), B_c^*(2^3S_1)) + b + \bar{c}, \tag{7}$$

$$q + \bar{q} \to B_c(B_c^*, B_c(2^1S_0), B_c^*(2^3S_1)) + b + \bar{c}, \tag{8}$$

with $q = g$, u, d, s. Some typical Feynman diagrams for calculating the partonic cross sections are shown in Fig. 2. In the analytical and numerical calculations, we use the well-established package Feynman diagram calculation (FDC) [59], which employs the standard projection method [60] to deal with the amplitudes.

III. NUMERICAL RESULTS AND DISCUSSIONS

The input parameters in the calculation are taken as follows. The fine structure constant is fixed as $\alpha = 1/137$. $m_b = 4.8$ GeV, $m_c = 1.5$ GeV and $M_{B_c} = m_b + m_c$. The one-loop running strong coupling constant is employed. The renormalization scale is set to be the transverse mass of the B_c meson, $\mu = \sqrt{M_{B_c}^2 + p_t^2}$ with p_t being its transverse momentum. The LDMEs $\langle \mathcal{O}^{B_c}[n]\rangle$
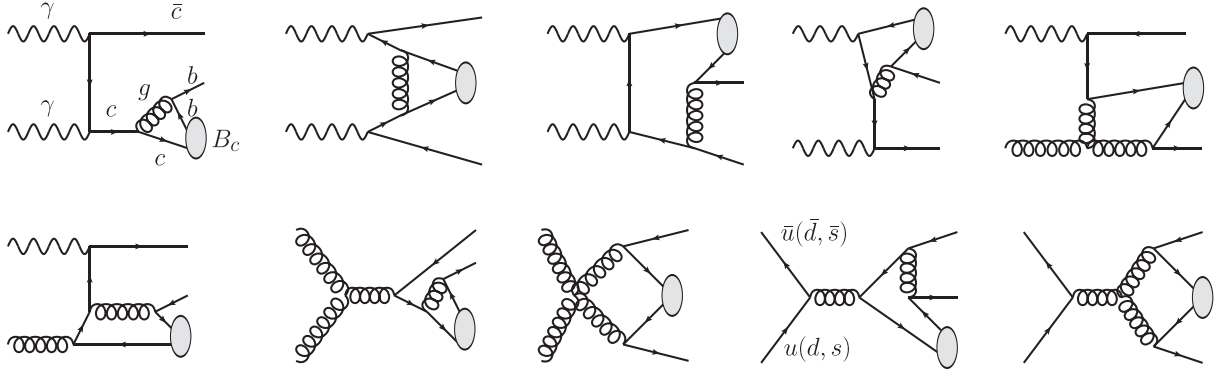
FIG. 2. Some typical Feynman diagrams for calculating the partonic cross section $\hat{\sigma}$ of B_c photoproduction at e^+e^- collider. The diagrams are drawn by JaxoDraw [61].

are related to the wave function at the origin, e.g., $\langle \mathcal{O}^{B_c}[n] \rangle \approx N_c |R_S(0)|^2/(2\pi)$, with $|R_{1S}(0)|^2 = 1.642 \text{ GeV}^3$ and $|R_{2S}(0)|^2 = 0.983 \text{ GeV}^3$ [62,63].

Table I lists the integrated cross section of the photoproduction of B_c under three typical collision energies, both for the LBS photon and WWA photon. It is shown from the table that all cross sections become larger with the increment of collision energy. The cross sections via LBS photon are much larger than those of WWA photon. This is due to the quite different spectra functions of them as shown in Fig. 1. We can also see that the production rate of the vector meson B_c^* are much larger than those of the scalar B_c. Since the excited states decay to the ground state with almost 100% probability, they will greatly increase the

production of B_c. Taking as example the integrated luminosity of future e^+e^- collider to be $\mathcal{O}(10^4)\text{ fb}^{-1}$ and considering the feed-down contributions from excited B_c states, we shall have about $3.3 \times 10^6 (1.3 \times 10^5) B_c$ mesons to be generated via LBS (WWA) photons under collision energy $\sqrt{s} = 250$ GeV. Thus the photoproduction of B_c at future e^+e^- colliders provides good opportunity to study B_c meson.

Table II shows the contributions from different channels for the LBS photon. With the increase of $\sqrt{s}$, the cross section of direct photoproduction channel [Eq. (6)] decreases, while those of the other two channels become larger. At $\sqrt{s} = 250$ GeV, the $\gamma + \gamma$ channel provides the largest production and the single-resolved photoproduction $\gamma + g$ also gives significant contributions. With the increment of the collision energy, the channel $\gamma + g$ becomes dominant. Consequently for the LBS photon, the resolved photoproduction channels of B_c at future e^+e^- colliders should be taken into account.

The situations are quite different for the WWA photon, as shown in Table III. The cross sections of all the three channels become larger when increasing the collision energy. The $\gamma + \gamma$ channels are always dominant while contributions of other two channels are very small or even negligible.

Figure 3 presents the transverse momentum distributions of B_c photoproduction. All the distributions have a peak around several GeV of p_t and decrease logarithmically in

TABLE I. The integrated cross sections (in unit of fb) for the photoproduction of B_c via the LBS photon and the WWA photon (in brackets), respectively. Three typical collision energies are taken and the cut $p_t > 1$ is imposed. Three channels of Eqs. (6)–(8) have been summed up.

$\sqrt{S}$ (GeV)	250	500	1000
σ_{B_c}	33.50(0.73)	38.74(1.59)	55.99(3.04)
$\sigma_{B_c^*}$	175.06(7.14)	177.49(14.09)	240.69(24.82)
$\sigma_{B_c(2^1S_0)}$	20.05(0.44)	23.19(0.95)	33.52(1.82)
$\sigma_{B_c^*(2^3S_1)}$	104.80(4.27)	106.26(8.43)	144.09(14.86)

TABLE II. The integrated cross sections (in units of fb) of different channels of the photoproduction of B_c via the LBS photon. Three typical collision energies, 250(500, 1000) GeV, are taken and the cut $p_t > 1$ is imposed.

Channels	$\gamma + \gamma$	$\gamma + g$	$q + \bar{q}$
σ_{B_c}	20.28(10.74, 4.92)	12.89(27.10, 48.70)	0.33(0.90, 2.37)
$\sigma_{B_c^*}$	114.90(54.93, 23.42)	59.03(120.05, 211.15)	1.14(2.51, 6.12)
$\sigma_{B_c(2^1S_0)}$	12.14(6.43, 2.95)	7.72(16.22, 29.15)	0.20(0.54, 1.42)
$\sigma_{B_c^*(2^3S_1)}$	68.78(32.88, 14.02)	35.34(71.87, 126.41)	0.68(1.50, 3.66)

TABLE III. The integrated cross sections (in units of fb) of different channels of the photoproduction of B_c via the WWA photon. Three typical collision energies, 250(500, 1000) GeV, are taken and the cut $p_t > 1$ is imposed.

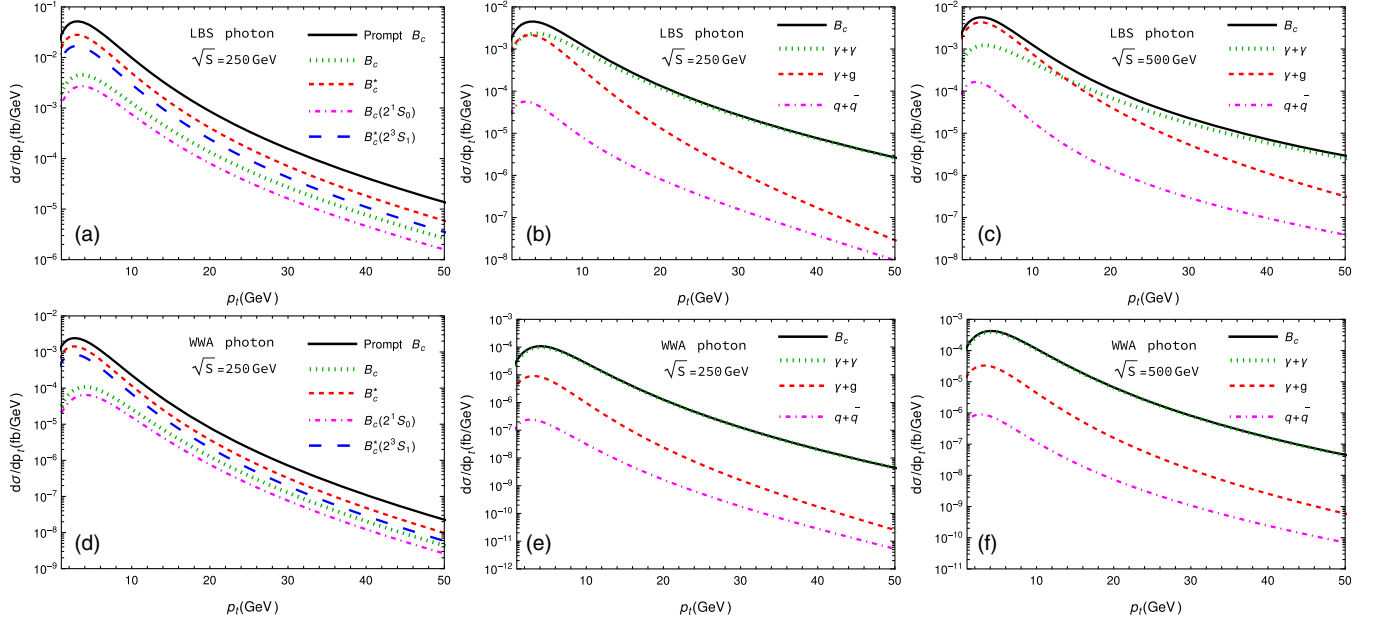| Channels	$\gamma + \gamma$	$\gamma + g$	$q + \bar{q}$
σ_{B_c}	0.68(1.33, 2.37)	0.05(0.19, 0.58)	0.001(0.005, 0.017)
$\sigma_{B_c^*}$	6.89(13.18, 22.11)	0.24(0.89, 2.64)	0.007(0.02, 0.06)
$\sigma_{B_c(2^1S_0)}$	0.41(0.83, 1.46)	0.03(0.11, 0.35)	0.0008(0.003, 0.01)
$\sigma_{B_c^*(2^3S_1)}$	4.13(7.89, 13.24)	0.14(0.53, 1.58)	0.004(0.013, 0.036)

FIG. 3. The p_t distributions for B_c photoproduction. (a,d): p_t distributions of four B_c states and "prompt B_c" means production of the ground B_c after including the feed-down contributions from excited states with 100% decay probability to it. (b,c,e,f): p_t distributions for the channels in Eqs. (6)–(8) of the ground B_c production.

the large region. From Figs. 3(b)–(c), we can see that the single resolved channel $\gamma + g$ give important contributions in relative small p_t region. In real experiments, there maybe not enough B_c events in large p_t region to make well measurements. Thus the single resolved photoproduction should be included in the calculation of B_c photoproduction. For the WWA photon, the direct photoproduction channel $\gamma + \gamma$ is always primarily dominant in whole p_t region.

Figure 4 presents the photoproduction in terms of the rapidity(y) distributions of final B_c mesons. There are wide plateaux within $|y| < 2.5$ for the LBS photoproduction

at $\sqrt{s} = 250$ GeV, while the curves carved in at $\sqrt{s} = 500$ GeV. This is because with the increase of collision energy, the contribution of $\gamma + g$ channel becomes dominant. The rapidity distribution of WWA photoproduction look ordinary compared with the LBS case.

Take $\sqrt{s} = 250$ GeV as example, we estimate theoretical uncertainties induced by the heavy quark masses and the renormalization scale. Table IV presents the uncertainties from the variation of charm quark mass where we take $m_c = 1.5 \pm 0.1$ GeV with $m_b = 4.8$ GeV and $\mu = \sqrt{M_{B_c}^2 + p_t^2}$. Table V shows the uncertainties from
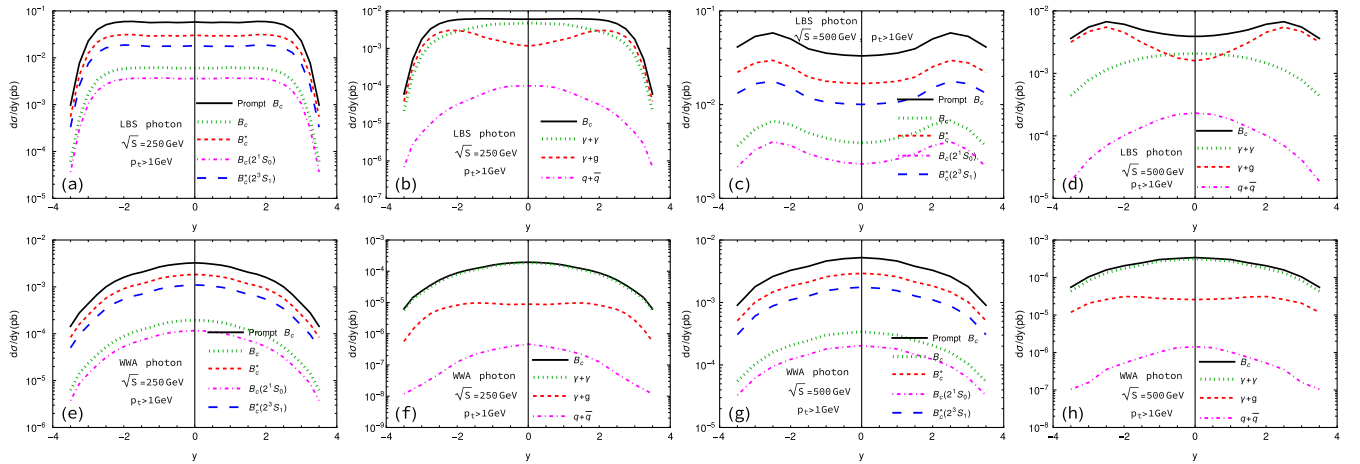

FIG. 4. The rapidity (y) distributions for B_c photoproduction. (a,c,e,g): y distributions of four B_c states and "prompt B_c" means production of the ground B_c after including the feed-down contributions from excited states with 100% decay probability to it. (b,d,f, h): y distributions for three channels in Eqs. (6)–(8) of the ground B_c production.

TABLE IV. Variations of the integrated cross sections (in unit of fb) by m_c for the photoproduction of B_c via the LBS photon and WWA photon (in brackets) at $\sqrt{s} = 250$ GeV, respectively. The cut $p_t > 1$ is imposed and three channels of Eqs. (6)–(8) have been summed up.

m_c (GeV)	1.4	1.5	1.6
σ_{B_c}	41.09(0.92)	33.50(0.73)	27.64(0.59)
$\sigma_{B_c^*}$	211.81(8.73)	175.06(7.14)	146.46(5.90)
$\sigma_{B_c(2^1S_0)}$	24.60(0.55)	20.05(0.44)	16.55(0.35)
$\sigma_{B_c^*(2^3S_1)}$	126.80(5.23)	104.80(4.27)	87.68(3.53)

TABLE V. Variations of the integrated cross sections (in units of fb) by m_b for the photoproduction of B_c via the LBS photon and the WWA photon (in brackets) at $\sqrt{s} = 250$ GeV, respectively. The cut $p_t > 1$ is imposed and three channels of Eqs. (6)–(8) have been summed up.

m_b (GeV)	4.6	4.8	5.0
σ_{B_c}	38.72(0.87)	33.50(0.73)	29.16(0.61)
$\sigma_{B_c^*}$	201.84(8.59)	175.06(7.14)	152.76(5.97)
$\sigma_{B_c(2^1S_0)}$	23.18(0.52)	20.05(0.44)	17.45(0.37)
$\sigma_{B_c^*(2^3S_1)}$	120.83(5.14)	104.80(4.27)	91.45(3.57)

TABLE VI. Variations of the integrated cross sections (in unit of fb) by $\mu = \mathcal{C}\sqrt{M_{B_c}^2 + p_t^2}$ with $\mathcal{C} = 0.5$, 1, 2, for the photoproduction of B_c via the LBS photon and WWA photon (in brackets) at $\sqrt{s} = 250$ GeV, respectively. The cut $p_t > 1$ is imposed and three channels of Eqs. (6)–(8) have been summed up.

$\mathcal{C}$	0.5	1.0	2.0
σ_{B_c}	45.69(1.07)	33.50(0.73)	25.77(0.53)
$\sigma_{B_c^*}$	243.06(10.68)	175.06(7.14)	133.30(5.15)
$\sigma_{B_c(2^1S_0)}$	27.35(0.64)	20.05(0.44)	15.43(0.32)
$\sigma_{B_c^*(2^3S_1)}$	145.51(6.39)	104.80(4.27)	79.80(3.08)

$m_b = 4.8 \pm 0.2$ GeV with $m_c = 1.5$ GeV and $\mu = \sqrt{M_{B_c}^2 + p_t^2}$. Table VI is for $\mu = \mathcal{C}\sqrt{M_{B_c}^2 + p_t^2}(\mathcal{C} = 0.5, 1, 2)$ with $m_c = 1.5$ GeV and $m_b = 4.8$ GeV. We

see that slight variation of the heavy quark mass can result in substantial change of the cross sections. A strong dependence on the renormalization scale indicates it is maybe large that the next-to-leading order and higher orders of corrections in α_s.

IV. SUMMARY

In this work, we have investigated the photoproduction of B_c, B_c^*, $B_c(2^1S_0)$, and $B_c^*(2^3S_1)$ at future e^+e^- colliders, where two sources of initial photons can be realized, i.e., the LBS photon and the WWA photon. Besides the direct photon-photon fusion, we specially consider the resolved photoproduction mechanisms that are generalized via the channels of Eqs. (7) and (8), which are lack in previous studies. Numerical results show that the single resolved photoproduction channel [Eq. (7)] can give sizable and even dominant contributions under certain collision configurations, e.g., the LBS photoproduction at $\sqrt{s} = 500$ GeV. Considering the excited states of B_c could decay to the ground state with almost 100% probability, they shall be important sources of B_c production. If setting the integrated luminosity of future e^+e^- collider to be $\mathcal{O}(10^4)$ fb^{-1} and considering the feed-down contributions from the excited B_c states, we shall have about 3.3×10^6 (1.3×10^5) B_c meson events to be generated via the LBS (WWA) photons under the collision energy $\sqrt{s} = 250$ GeV. However, the leading-order calculations in α_s of the cross section have large dependence on the heavy quark masses and the renormalization scale, which means corrections of higher orders maybe substantial. We would like to leave them for future study. Nevertheless, we could expect that future e^+e^- colliders to be good platforms for investigating the B_c meson properties.

[1] F. Abe *et al.* (CDF Collaboration), Phys. Rev. Lett. **81**, 2432 (1998).

[2] F. Abe *et al.* (CDF Collaboration), Phys. Rev. D **58**, 112004 (1998).

[3] G. Aad *et al.* (ATLAS Collaboration), Phys. Rev. Lett. **113**, 212004 (2014).

[4] A. M. Sirunyan *et al.* (CMS Collaboration), Phys. Rev. Lett. **122**, 132001 (2019).

[5] R. Aaij *et al.* (LHCb Collaboration), Phys. Rev. Lett. **122,** 232001 (2019).

[6] C.-H. Chang and Y.-Q. Chen, Phys. Rev. D **48,** 4086 (1993).

[7] C.-H. Chang, Y.-Q. Chen, G.-P. Han, and H.-T. Jiang, Phys. Lett. B **364,** 78 (1995).

[8] K. Kolodziej, A. Leike, and R. Ruckl, Phys. Lett. B **355,** 337 (1995).

[9] A. V. Berezhnoy, A. K. Likhoded, and M. V. Shevlyagin, Phys. At. Nucl. **58,** 672 (1995).

[10] C.-H. Chang, Y.-Q. Chen, and R. J. Oakes, Phys. Rev. D **54,** 4344 (1996).

[11] A. V. Berezhnoy, V. V. Kiselev, and A. K. Likhoded, Z. Phys. A **356,** 79 (1996).

[12] S. P. Baranov, Phys. Rev. D **55,** 2756 (1997).

[13] S. P. Baranov, Phys. Rev. D **56,** 3046 (1997).

[14] K.-m. Cheung, Phys. Lett. B **472,** 408 (2000).

[15] C.-H. Chang and X.-G. Wu, Eur. Phys. J. C **38,** 267 (2004).

[16] C.-H. Chang, J.-X. Wang, and X.-G. Wu, Phys. Rev. D **70,** 114019 (2004).

[17] C.-H. Chang, C.-F. Qiao, J.-X. Wang, and X.-G. Wu, Phys. Rev. D **71,** 074012 (2005).

[18] C.-H. Chang, C.-F. Qiao, J.-X. Wang, and X.-G. Wu, Phys. Rev. D **72,** 114009 (2005).

[19] C.-H. Chang, C. Driouichi, P. Eerola, and X. G. Wu, Comput. Phys. Commun. **159,** 192 (2004).

[20] C.-H. Chang, J.-X. Wang, and X.-G. Wu, Comput. Phys. Commun. **174,** 241 (2006).

[21] X.-Y. Wang and X.-G. Wu, Comput. Phys. Commun. **183,** 442 (2012).

[22] H.-Y. Bi, R.-Y. Zhang, H.-Y. Han, Y. Jiang, and X.-G. Wu, Phys. Rev. D **95,** 034019 (2017).

[23] G. Chen, C.-H. Chang, and X.-G. Wu, Phys. Rev. D **97,** 114022 (2018).

[24] A. V. Berezhnoy, I. N. Belov, A. K. Likhoded, and A. V. Luhinsky, Mod. Phys. Lett. A **34,** 1950331 (2019).

[25] X.-C. Zheng, C.-H. Chang, X.-G. Wu, J. Zeng, and X.-D. Huang, Phys. Rev. D **101,** 034029 (2020).

[26] A. Abada *et al.* (FCC Collaboration), Eur. Phys. J. Special Topics **228,** 261 (2019).

[27] C. S. Group, arXiv:1809.00285.

[28] M. Dong *et al.* (CEPC Study Group Collaboration), arXiv:1811.10545.

[29] G. Aarons *et al.* (ILC Collaboration), arXiv:0709.1893.

[30] J. Erler, S. Heinemeyer, W. Hollik, G. Weiglein, and P. M. Zerwas, Phys. Lett. B **486,** 125 (2000).

[31] Z. Yang, X.-G. Wu, G. Chen, Q.-L. Liao, and J.-W. Zhang, Phys. Rev. D **85,** 094015 (2012).

[32] G. Chen, X.-G. Wu, Z. Sun, X.-C. Zheng, and J.-M. Shen, Phys. Rev. D **89,** 014006 (2014).

[33] G. Chen, X.-G. Wu, Z. Sun, S.-Q. Wang, and J.-M. Shen, Phys. Rev. D **88,** 074021 (2013).

[34] Z. Sun, X.-G. Wu, G. Chen, J. Jiang, and Z. Yang, Phys. Rev. D **87,** 114008 (2013).

[35] G. Chen, X.-G. Wu, H.-B. Fu, H.-Y. Han, and Z. Sun, Phys. Rev. D **90,** 034004 (2014).

[36] Z. Sun, X.-G. Wu, G. Chen, Y. Ma, H.-H. Ma, and H.-Y. Bi, Phys. Rev. D **89,** 074035 (2014).

[37] Z. Sun, X.-G. Wu, and H.-F. Zhang, Phys. Rev. D **92,** 074021 (2015).

[38] Z.-G. He and B. A. Kniehl, CERN Yellow Rep. Monogr. **3,** 89 (2020).

[39] X.-J. Zhan and J.-X. Wang, Eur. Phys. J. C **80,** 740 (2020).

[40] X.-J. Zhan and J.-X. Wang, Chin. Phys. C **45,** 023112 (2021).

[41] X.-J. Zhan, X.-G. Wu, and X.-C. Zheng, J. High Energy Phys. 09 (2022) 050.

[42] Z. Yang, X.-G. Wu, and X.-Y. Wang, Comput. Phys. Commun. **184,** 2848 (2013).

[43] X.-C. Zheng, C.-H. Chang, and Z. Pan, Phys. Rev. D **93,** 034019 (2016).

[44] A. V. Berezhnoy, A. K. Likhoded, A. I. Onishchenko, and S. V. Poslavsky, Nucl. Phys. **B915,** 224 (2017).

[45] X.-C. Zheng, C.-H. Chang, T.-F. Feng, and Z. Pan, Sci. China Phys. Mech. Astron. **61,** 031012 (2018).

[46] X.-C. Zheng, C.-H. Chang, and T.-F. Feng, Sci. China Phys. Mech. Astron. **63,** 281011 (2020).

[47] Z.-Y. Zhang, X.-C. Zheng, and X.-G. Wu, Eur. Phys. J. C **82,** 246 (2022).

[48] Z. Yang, X.-C. Zheng, and X.-G. Wu, Comput. Phys. Commun. **281,** 108503 (2022).

[49] Z.-Q. Chen, H. Yang, and C.-F. Qiao, Phys. Rev. D **102,** 016011 (2020).

[50] H. Yang, Z.-Q. Chen, and C.-F. Qiao, Phys. Rev. D **105,** 094014 (2022).

[51] S. Frixione, M. L. Mangano, P. Nason, and G. Ridolfi, Phys. Lett. B **319,** 339 (1993).

[52] M. Klasen, B. A. Kniehl, L. N. Mihaila, and M. Steinhauser, Phys. Rev. Lett. **89,** 032001 (2002).

[53] R. Li and K.-T. Chao, Phys. Rev. D **79,** 114020 (2009).

[54] G. T. Bodwin, E. Braaten, and G. P. Lepage, Phys. Rev. D **51,** 1125 (1995); **55,** 5853(E) (1997).

[55] I. F. Ginzburg, G. L. Kotkin, V. G. Serbo, and V. I. Telnov, Nucl. Instrum. Methods **205,** 47 (1983).

[56] V. I. Telnov, Nucl. Instrum. Methods Phys. Res., Sect. A **294,** 72 (1990).

[57] For simplicity, here only formulas for the ground-state B_c meson are presented and those for the excited states are similar.

[58] M. Gluck, E. Reya, and I. Schienbein, Phys. Rev. D **60,** 054019 (1999); **62,** 019902(E) (2000).

[59] J.-X. Wang, Nucl. Instrum. Methods Phys. Res., Sect. A **534,** 241 (2004).

[60] G. T. Bodwin and A. Petrelli, Phys. Rev. D **66,** 094011 (2002); **87,** 039902(E) (2013).

[61] D. Binosi and L. Theussl, Comput. Phys. Commun. **161,** 76 (2004).

[62] E. J. Eichten and C. Quigg, Phys. Rev. D **49,** 5845 (1994).

[63] E. J. Eichten and C. Quigg, Phys. Rev. D **52,** 1726 (1995).